Research article

Measuring residence time distributions of wood chips in a screw conveyor reactor

Charles Chamberlin*, David Carter, Arne Jacobson

Schatz Energy Research Center, Humboldt State University, Arcata, CA 95521, United States

ABSTRACT

In rotating screw conveyors both the average and the distribution of the residence time influence the extent and the uniformity of the transformation. Experimenters have applied two distinct experimental approaches to obtain the residence time distribution of granular solids in longitudinal reactors: 1) measuring the mass flow rate of product at the exit from the reactor in response to a step change (either positive or negative) in the mass flow rate of feedstock into the reactor or 2) measuring the appearance of a tracer in the flow exiting the reactor in response to either a pulse or a step change addition of tracer in the inlet. We found that all three methods reveal residence time distributions that are approximately normal (i.e., symmetrical and bell-shaped), but the distribution estimated from the pulse input of tracer exhibited a long trailing tail that was not detectable in either the positive or negative step changes. Second, we demonstrated that a normal probability plot proved valuable in displaying and analyzing the residence time distribution obtained by the pulse addition of tracer. Finally, we observed that all three methods yielded mean residence times that consistently differed from the nominal values. The positive step change averaged 8% shorter, the pulse addition of tracer averaged 7% longer, and the negative step change averaged 60% longer.

1. Introduction

Rotating screw conveyors are widely used to transport granular solids through heaters, coolers, dryers, torrefiers, gasifiers and other reactors where controlling the residence time of the particulates is important. Since the degree of physical and chemical transformation of the granular solids depends on the residence time in the reactor at the target operating conditions, both the average residence time and the distribution of the residence time influence the extent and the uniformity of the transformation.

In an ideal system, the successive flights of the rotating screw conveyor sweep the solids steadily forward at a rate controlled by the rotation rate and flight length of the screw, allowing computation of the ideal or nominal residence time. However, in real systems some particles evade forward transport by passing through the flight clearance (i.e., the gap between the screw and the shell), stepping backwards to a previous screw blade or flight. If the reactor is sufficiently full, then other particles can cascade backwards over the screw axis (or in the case of axle-less screws, over the screw ribbon) into a previous flight. Both of these non-ideal transport processes result in axial dispersion or longitudinal mixing of the solids, observed residence times that exceed the ideal, and variability of the properties of the reactor product.

Levenspiel and Smith [6] characterized non-ideal transport of fluids in longitudinal reactors using solutions to the advection-diffusion equation, and their approach provides the dominant modeling framework for the analysis of resident time distribution. This framework has been applied to the transport of granular solids in screw conveyors by Nachenius et al. [8] and Waje et al. [10], in twin-screw extruders by Kumar et al. [5], and in rotary drums by Bongo Njeng et al. [3] and Colin et al. [4]. These models characterize the residence time distribution using one set of two alternative pairs of parameters: a) the mean and standard deviation of the residence time or b) the mean longitudinal transport velocity and the longitudinal dispersion coefficient. Both sets of parameters are estimated empirically from observed residence time distributions.

Experimenters have applied two distinct experimental approaches to obtain the residence time distribution of granular solids in longitudinal reactors: 1) measuring the mass flow rate of product at the exit from the reactor in response to a step change (either positive or negative) in the mass flow rate of feedstock into the reactor or 2) measuring the appearance of a tracer in the flow exiting the reactor in response to either a pulse or a step change addition of tracer in the inlet. The first method was employed by Nachenius et al. [8] using a negative step change in the inlet mass flow rate. The second method was

---

* Corresponding author.
  E-mail addresses: charles.chamberlin@humboldt.edu (C. Chamberlin), david.carter@humboldt.edu (D. Carter), arne.jacobson@humboldt.edu (A. Jacobson).

implemented by Waje et al. [10] adding a pulse of dyed solids to the inlet. Both works estimated the mean and standard deviation of the residence time distribution following the method described by Levenspiel and Smith [6] and Levenspiel [7].

In the negative step change experiments of Nachenius et al. [8] the observed mean residence times were consistently longer than the ideal residence times (i.e., computed from the length, pitch, and rotational frequency of the screw), sometimes by as much as 50%. This discrepancy was statistically well explained by the degree of filling of the reactor, with greater degree of filling strongly associated with increases in the observed mean residence time relative to the ideal.

In contrast, the pulse addition of tracer experiments reported by Waje et al. [10] showed observed mean residence times from 250% to 350% longer than the ideal residence times. Although these large differences were not statistically associated with the degree of filling, the authors ascribed the effect to backflow.

There are three objectives of the analysis presented in this article. First, compare the residence time distributions and their properties obtained by three alternative experimental methods: 1) a pulse input of tracer, 2) a positive step change in the reactor mass input rate, and 3) a negative step change in the reactor mass input rate. Second, compare alternative methods describing the residence time distribution and for estimating the mean and standard deviation of the residence time. And finally, compare the estimated mean residence times to the nominal or ideal residence times.

2. Materials and experimental methods

The feedstock for the experiments described below was chipped and screened Douglas fir tops and branches obtained during normal forest harvesting operations. All material passed through a 3.81 mm (1.5 in.) screen. Since the feedstock for each of the four experiments was obtained from a single well-mixed pile, we collected a single representative sample of feedstock from this pile for measuring the particle size distribution by sieving. The results are presented in Table 1 and show 87% of the particles are between 3.99 and 26.7 mm. The bulk density of the feedstock was 180 kg/m^3 (11 lb/ft^3).

The tracer used in these experiments was the feedstock dyed with red ink. The ink, marketed for refilling inkjet printer cartridges, was sprayed onto the feedstock by hand and air dried. In the reactor, the feedstock was not exposed to substances that would destabilize the ink during the experiment.

All of these experiments were conducted in a torrefier reactor produced by Norris Thermal Technologies (Tippecanoe, Indiana) that incorporates a Spiraoule® electrically heated, shaftless screw conveyor (ETIA, France). During these experiments, the screw conveyor was not heated and the lid for the reactor compartment was removed. Fig. 1 provides a schematic diagram of the part of the torrefier system used here. Feedstock is added to the input hopper and is fed into the torrefier

reactor by a 6-chamber, rotary airlock at a rate controlled by the speed setting of motor M1. Each chamber of the airlock has a volume of 273 cm^3. The feedstock is moved through the reactor by the shaftless screw conveyor at a rate controlled by the speed setting of motor M2. The conveyor was 166 cm (65.5 in.) long and had a diameter of 13.3 cm (5.25 in.) with a pitch of 5.08 cm (2.0 in.) and a screw blade width of 4.45 cm (1.75 in.). Material exits the reactor through an output airlock that is identical to the one used at the inlet. The speed setting for motor M3 controls the output rate of the solid product. During normal torrefier operation the screw is heated and syngas is extracted through the syngas outlet.

In each of the four residence time experiments that were conducted, the reactor was initially empty and the motor speeds for the two airlocks and the screw conveyor were fixed at the values presented below in the results and discussion. In order to reduce or avoid backward transport of particles in the reactor due to over-filling, longer residence time runs required reduction of the mass flow rate through the system. Fig. 2 presents the ideal time pattern of the mass flow rate at the inlet of the input air airlock (dotted line) and at the exit from the output airlock (solid line). At time t = 0, feedstock was added to the input hopper and soon began to enter the reactor, beginning the positive step change in the input rate. When the hopper feedstock level became low, additional feedstock was added. When the mass flow rate exiting the output airlock reached steady state (i.e., the average over time became approximately constant and the input and output mass flow rates became equal) and the feedstock hopper became empty, the positive step (rising arm) portion of the experiment was concluded and the pulse of tracer was added, beginning that portion of the experiment. After all the tracer had entered the input airlock, feedstock was again added to the hopper and continued to be added as necessary. When the material exiting the output airlock no longer contained tracer, the hopper was emptied and no additional feedstock entered the reactor, beginning the negative step change in the input rate. When the mass flow rate exiting the output airlock became consistently zero, the experiment was ended.

Mass flow rates were measured at the exit from the output airlock by collecting all of the material exiting the reactor over a measured time interval of either 30 or 60 s. The material was collected in a tared container, the container with material was then weighed on a 0.1 g balance, and the result was recorded. Collected material containing tracer (i.e., labeled feedstock) was transferred to a labeled plastic bag, sealed, and stored for later analysis.

After the conclusion of the experiment, each of the bagged samples containing tracer material was re-weighed and screened through a 0.236 mm (0.093 in.) sieve to eliminate fines to facilitate sorting by hand. The remaining material was then sorted by hand to separate the tracer from the feedstock and then weighed and recorded.

3. Theory and analytical method

The theory and methods described here for estimating the mean and standard deviation of the residence time are based on those originally developed by Levenspiel and Smith [6] and recently applied by Nachenius et al. [8] and Waje et al. [10] to the transport of granular solids by screw conveyors. Two novel variations on these methods are highlighted below (i.e., a graphical and linear regression method using normal probability plots and the use of the median residence time to estimate the mean).

The theoretical or ideal residence time in the screw conveyor (τ_{sc}) can be computed from the length of the conveyor (L), the length of the screw flight or pitch (p), and the screw conveyor (i.e., M2) rotation rate (ω_{sc}) (see Fig. 1):

$$\tau_{sc} = \frac{L}{p \cdot \omega_{sc}} \tag{1}$$

This ideal screw conveyor residence represents the amount of time required for a parcel of feedstock entering the reactor to arrive at the

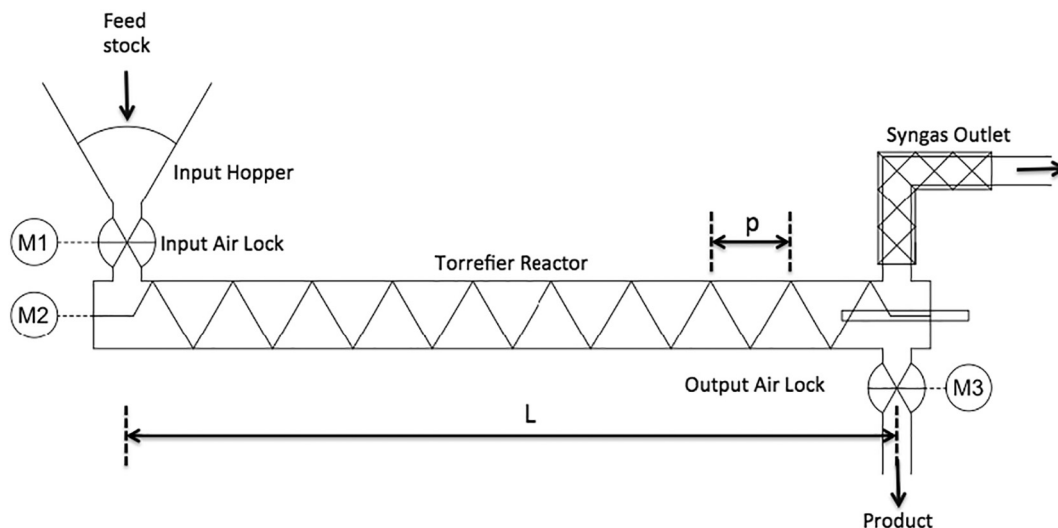**Table 1**
Particle size distribution of feedstock.

Lower size limit (mm)	Upper size limit (mm)	wt (g)	% wt
50.8	–	5.3	1%
38.1	50.8	6.1	1%
26.7	38.1	10.4	2%
18.8	26.7	88.2	14%
13.3	18.8	34.9	6%
11.1	13.3	156.0	25%
7.94	11.1	109.3	18%
5.59	7.94	86.3	14%
3.99	5.59	74.6	12%
2.79	3.99	17.7	3%
1.00	2.79	18.1	3%
0	1.00	16.3	3%
Total		623.2	100%

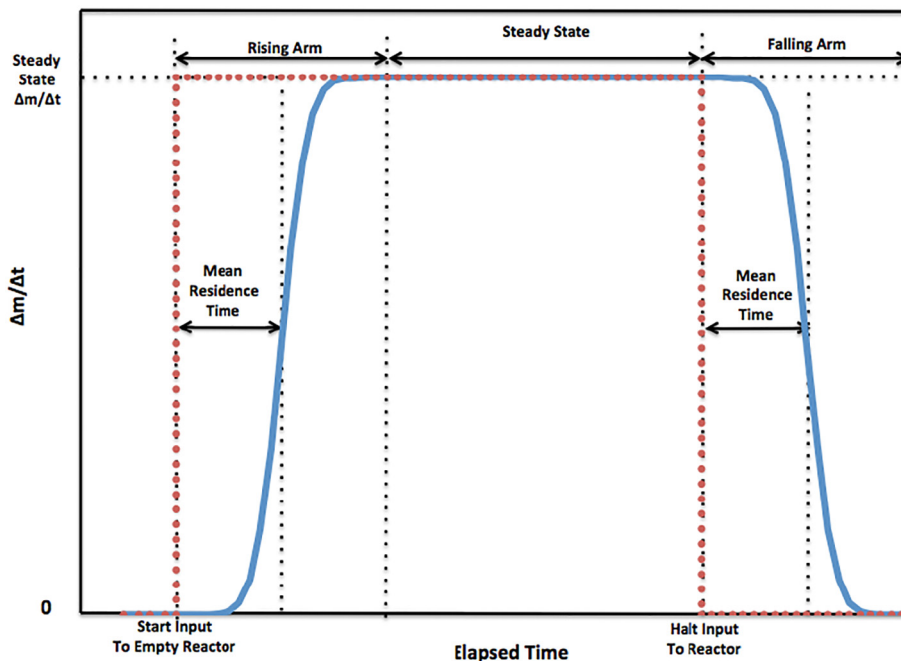**Fig. 1.** Diagram of Norris Thermal Technologies torrefier.

Fig. 2. Ideal time profiles of input (dotted line) and exit (solid line) mass flow rates.

exit. In the ideal case, all of the feedstock entering at a given time would exit the reactor together at exactly τ_{sc} later.

However, the passage of the solids through the input and output airlocks also contributes to the overall reactor residence time (τ_{ideal}). Solids enter one of the six partitions or bins making up each airlock (as shown in Fig. 1), the airlock rotates 180° or 0.5 revolution, and the solids exit the airlock. So the additional residence time equals 50% of the time for one revolution. For rotation rates of ω_{in} and ω_{out} for the inlet and outlet airlocks, the ideal residence time for the overall reactor can be computed as:

$$\tau_{ideal} = \frac{0.5}{\omega_{in}} + \frac{L}{p \cdot \omega_{sc}} + \frac{0.5}{\omega_{out}} \tag{2}$$

In actual experiments, parcels of feedstock that enter the reactor at the same time do not all exit at the same time. This distribution in residence time or arrival time is the focus of this work. The results from each experiment were used to estimate the mean, $\bar{t}$, and the standard deviation, S_t, of the residence or arrival time (t_i) based on the observed

response to A) the positive step change in input at the start of the experiment (i.e., the change from zero to a constant input rate), B) the pulse addition of the tracer during the steady state section of the experiment, and C) the negative step change at the end of the experiment (i.e., the change from constant input rate to zero). The statistical estimators applied to each of these three distinct datasets are subscripted accordingly (i.e., $\bar{t}_A$ and $S_{t,\,A}$ are the estimators for the mean and standard deviation of the residence time based on the positive step change data and $\bar{t}_C$, and $S_{t,\,C}$ are the corresponding estimators for the negative step change data). The analysis of the pulse addition results involved applying three alternative estimators of the mean residence time (i.e., $\bar{t}_{B,1}$, $\bar{t}_{B,2}$, and $\bar{t}_{B,3}$) and two alternative estimators of the standard deviation of the residence time (i.e., $S_{t,\,B,\,1}$ and $S_{t,\,B,\,2}$).

The addition of feedstock through the inlet airlock (and the removal of product through the outlet airlock) occurs as each of the six chambers rotates into a position where the material in the chamber can begin emptying into the reactor and should be fully empty when the chamber is pointed directly down. So material exits as the airlock rotates 0.167

revolution and material enters the reactor at a rate of 6. ω_{in} (chambers per min). Simultaneously, the screw conveyor is advancing at a speed of 1 flight per revolution or ω_{sc} flights per minute. The ratio of these two rates yields the expected number of chambers emptied into each flight:

$$q_{in} = \frac{6 \cdot \omega_{in}}{\omega_{sc}} \tag{3a}$$

$$q_{out} = \frac{6 \cdot \omega_{out}}{\omega_{sc}} \tag{3b}$$

Following Waje et al. [11] the degree of fullness (α) quantifies the fraction of the reactor that is filled by solids during operation and can be estimated from the mass present within the reactor (m), the bulk density of the material (ρ_b), and the reactor volume (V):

$$\alpha = \frac{m}{\rho_b \cdot V} \tag{4}$$

The reactor volume was computed as the volume of the reactor chamber below the top of the screw. The bottom of the reactor below the centerline of the screw was semi-circular to match the diameter of the screw. The upper part of the chamber was rectangular in cross-section with a width equal to the diameter of the screw.

These three alternative experimental methods (i.e., positive step change, pulse addition, and negative step change) used different time periods of the same datasets.

Solids arrived at the reactor exit as a continuous but variable stream but were collected in a series of n discrete increments. At time t_{i-1}, one collection container was removed and a new, tared and empty container was inserted to begin collecting the solids output. The mass of the solids arriving at the reactor exit were collected in this container until time t_i, at which point the container was removed and replaced by a new collection container. The removed container was then weighed and the mass m_i of the solids collected over the time interval t_{i-1} to t_i was recorded. The mass flow rate of the solids exiting the reactor over that time interval was estimated as:

$$\dot{m}_i = \left(\frac{m_i}{t_i - t_{i-1}} \right) \tag{5}$$

and the mass flow rate of the tracer material exiting the reactor was estimated as:

$$\dot{m}_{t,i} = \left(\frac{m_{t,i}}{t_i - t_{i-1}} \right) \tag{6}$$

3.1. Positive step change

Using an adaptation of the method applied by Nachenius et al. [8] to their negative step change data, the residence time distribution was estimated from the response to the positive step change in the reactor mass input rate from zero to the steady state mass flow rate ($\dot{m}_{SS,A}$), assuming a normal distribution with a mean residence time of $\bar{t}_A$ and a standard deviation of $S_{t,A}$. The predicted exiting mass flow rate ($\widehat{\dot{m}_i}$) can be computed from the three parameters $\dot{m}_{SS,A}$, $\bar{t}_A$, and $S_{t,A}$ as:

$$\widehat{\dot{m}_i} = \dot{m}_{SS,A} \cdot F_N \left(\frac{t_i - \bar{t}_A}{S_{t,A}} \right) \tag{7}$$

where $F_N(z)$ is the cumulative normal distribution function of the standard normal deviate. Using nonlinear regression, values for $\dot{m}_{SS,A}$, $\bar{t}_A$, and $S_{t,A}$ are selected to minimize the sum of squared residuals between the observed $\dot{m}_i$ and the predicted $\widehat{\dot{m}_i}$. Solver in Excel® can be used to perform the nonlinear regression. The standard errors of $\dot{m}_{SS,A}$, $\bar{t}_A$, and $S_{t,A}$ can be computed from the Jacobian, i.e., the array of the first derivatives of the predicted mass flow rate with respect to each parameter evaluated for each data point [1].

3.2. Pulse addition of tracer

Following the approach of Levenspiel and Smith [6] and Waje et al. [10], the residence time distribution (RTD) function $f(t_i)$ for each tracer experiment was estimated as:

$$f(t_i) = \frac{m_{t,i}}{\sum_{i=1}^n m_{t,i}} \tag{8}$$

The associated cumulative RTD function ($F(t_j)$) for each tracer experiment was estimated as

$$F(t_j) = \frac{\sum_{i=1}^j m_{t,i}}{\sum_{i=1}^n m_{t,i}} \tag{9}$$

Based on the results from the pulse addition of tracer, the mean of the discrete random variable that is the residence or arrival time was estimated in three ways from the observed RTD function and the standard deviation of the residence time was estimated in two ways. The first way applied the estimators originally developed by Levenspiel and Smith [6], where the mean and standard deviation were estimated by using the RTD function as a probability distribution function for a discrete random variable (t_i):

$$\bar{t}_{B,1} = \sum_{i=1}^n f(t_i) \cdot t_i \tag{10}$$

$$S_{t,B,1} = \left[\sum_{i=1}^n f(t_i) \cdot (t_i - \bar{t}_{B,1})^2 \right]^{0.5} \tag{11}$$

In the second way which is novel, the cumulative RTD function was plotted as a normal probability plot, using t_j vs z and was fitted to a normal or Gaussian distribution. The ordinate axis variable is t_i and the abscissa axis variable is the expected standard normal deviate corresponding to the value of the cumulative RTD function (z), which can be conveniently approximated using a function developed by Tukey [9]:

$$z = 4.91 \cdot (F(t_i)^{0.14} - (1 - F(t_i))^{0.14}) \tag{12}$$

This approximation has less than a 1% error for values of $F(t_i)$ ranging from 0.001 to 0.999. Fig. 3 illustrates this method. To the extent that the cumulative RTD function can be approximated as a normal distribution, the normal probability plot will appear linear. Based on linear regression of t_j vs z, the intercept corresponds to the estimated mean residence time ($\bar{t}_{B,2}$), and the slope corresponds to the standard deviation of the residence time ($S_{t,B,2}$). Confidence intervals for the mean and standard deviation of the residence time can also be obtained from the regression results. So this method provides not only numerical
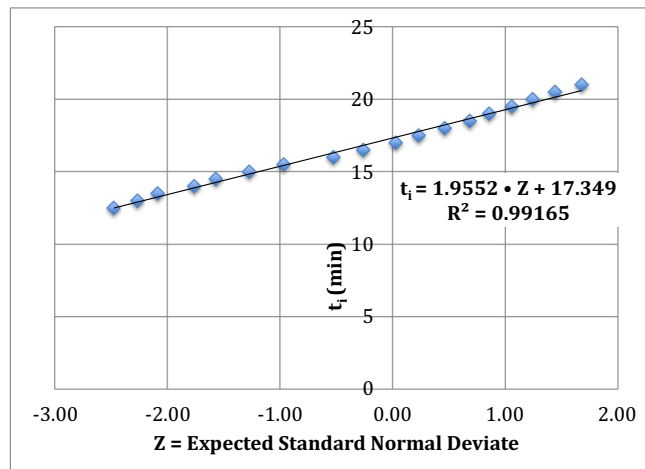
$$t_i = 1.9552 \cdot Z + 17.349$$
$$R^2 = 0.99165$$

Fig. 3. Example probability plot to determine mean and standard deviation of residence time.

estimates of the mean and standard deviation of the residence time but also standard errors for the estimated mean and standard deviation that can be used to produce confidence intervals plus a convenient graphical expression of the distribution that is well suited to comparing multiple sets of experimental results.

The third and final way of estimating the mean residence time was to use the observed cumulative residence time distribution ($F(t_j)$) to determine the median residence time ($\bar{t}_{B,3}$), since if the RTD is symmetrical (as the Gaussian or normal distribution is), then the median and the mean will be equal. Using the data points that bracket the 50th percentile (t_{j-1}, $F(t_{j-1}) < 50\%$ and t_j, $F(t_j) \geq 50\%$), the mean residence time was estimated by linear interpolation:

$$\bar{t}_{B,3} = t_{j-1} + \frac{(t_j - t_{j-1})}{(F(t_j) - F(t_{j-1}))} \cdot (0.5 - F(t_{j-1})) \tag{13}$$

3.3. Negative step change

Based on the method applied by Nachenius et al. [8], the residence time distribution was estimated from the response to the negative step change in the reactor mass input rate from the steady state mass flow rate ($\dot{m}_{SS,C}$) to zero, assuming a normal distribution with a mean residence time of $\bar{t}_C$ and a standard deviation of $S_{t,C}$. The predicted mass flow rate ($\widehat{m}_i$) can be computed from the three parameters $\dot{m}_{SS,C}$, $\bar{t}_C$, and $S_{t,C}$ as:

$$\widehat{m}_i = \dot{m}_{SS,C} \cdot \left(1 - F_N\left(\frac{t_i - \bar{t}_C}{S_{t,C}}\right)\right) \tag{14}$$

Using nonlinear regression, values for $\dot{m}_{SS,C}$, $\bar{t}_C$, and $S_{t,C}$ are selected to minimize the sum of squared residuals between the observed $\dot{m}_i$ and the predicted $\widehat{m}_i$, as described above for the positive step change. The standard errors of $\dot{m}_{SS,C}$, $\bar{t}_C$, and $S_{t,C}$ can be also be computed as described above for the positive step change. Note that although the estimated values for $\dot{m}_{SS,A}$ and $\dot{m}_{SS,C}$ may differ, the confidence interval for the difference in the values should include zero, indicating that the differences may be solely due to random variation.

4. Results and discussion

In this section, we report and discuss the results for four residence time experiments. We present the estimated ideal residence times, the residence time distribution results for the positive step, the pulse addition, and the negative step experiments, compare the residence time distribution parameters obtained by the alternative methods, and discuss the relative advantages and disadvantages of these alternative methods and estimators.

4.1. Ideal residence times

For each of the four experiments, the motor speeds on the input and output airlocks and on the screw conveyor were fixed. Table 2 presents the resulting airlock and screw conveyor rotation rates used in the residence time experiments and the ideal residence time computed using Eqs. (1) and (2). The experiments have been ordered from shortest to longest ideal residence time. The ideal residence times varied from 7.61 to 33.43 min. Note that the contribution of the airlocks to the total residence time in the system was particularly large in the final experiment. The residence time of the feedstock in the reactor was only 44% of the entire residence time within the system.

Also note that in all experiments the number of inlet airlock chambers emptied into each flight of the screw conveyor was always < 0.5 and sometimes as low as 0.14. So it is reasonable to expect that some flights may have received no material, which may at least in part explain the highly variable mass flow rates observed at the exit from the reactor, which will be discussed further in the next section.

Table 2
Ideal system residence times.

Experiment	1	2	3	4
ω_{in} (rpm)	0.308	0.210	0.183	0.053
ω_{out} (rpm)	0.493	0.493	0.183	0.053
ω_{sc} (rpm)	6.58	3.21	3.21	2.25
τ_{sc} (min)[a]	4.98	10.20	10.20	14.58
τ_{ideal} (min)	7.61	13.60	15.68	33.43
% of time in reactor[b]	65%	75%	65%	44%
q_{in} (chambers/flight)	0.28	0.39	0.34	0.14
q_{out} (chambers/flight)	0.45	0.92	0.34	0.14
α[c]	0.17	0.34	0.17	0.16

[a] For L = 166 cm (65.5 in.) and p = 5.08 cm (2.0 in.).
[b] % of time in reactor = τ_{sc} / τ_{ideal}.
[c] For ρ_b = 180 kg/m^3 and V = 0.026 m^3; m was estimated from the negative step change data.

Based on criteria proposed by Waje et al. [11], values of α between 0.1 and 0.3 indicate a medium degree of fullness while values above 0.3 indicate a high degree of fullness. Experiments 1, 3, and 4 show approximately equal degrees of fullness in the medium range (i.e., 0.16 to 0.17) while experiment 2 exhibits a degree of fullness about twice as large (i.e., 0.34) in the high range.

4.2. Steady state mass flow rate

Table 3 summarizes the statistical properties of the steady state mass flow rates observed during the experimental runs and provides the associated input airlock rotation rates and the ideal residence times for comparisons. The observations taken during the pulse addition of tracer were used to characterize the steady state period. Fig. 4 provides a normal probability plot of the observed mass flow rates for each of the four runs. The linear form of the plots indicates that the distributions are approximately normal for all of the runs, which is supported by the near equality of the sample mean and sample median flow rates reported in Table 3. There was considerable variability in the observed mass flow rate in all of the runs. For runs 1 through 3, which have ideal residence times below 16 min, the standard deviations of the steady state mass flow rates range from 12 to 14 g/min, while for run 4, which has a 33-minute ideal residence time, the standard deviation is only 7 g/min. These standard deviations correspond to coefficients of variation of ranging from 17% for run 1 to 58% for run 4.

As shown in Fig. 5, both the mean and standard deviation of the

Table 3
Steady state mass flow rate.

Parameter	1	2	3	4	Exp 1[a]	Exp 2[a]	Exp 3[a]
ω_{in} (rpm)	0.308	0.210	0.183	0.053	0.308	0.210	0.183
τ_{ideal} (min)	7.61	13.60	15.68	33.43	7.61	13.60	15.68
Steady state duration (min)	12	27.5	27	38	12	27.5	27
Sampling interval (min)	0.5	0.5	0.5	1.0	1.0	1.0	1.0
Sample size	24	56	55	56	12	28	27
Mean (g/min)	83.16	46.29	45.94	12.82	83.16	46.29	45.12
Standard deviation (g/min)	14.01	12.64	13.41	7.38	11.21	11.46	5.74
Coefficient of variation (%)	17%	27%	29%	58%	13%	25%	13%
SD (60s)/SD (30s)[b]					80%	91%	43%
Median (g/min)	83.92	45.52	46.20	12.50	89.32	43.78	44.7
Max (g/min)	101.92	75.28	90.00	27.80	94.72	69.24	57.1
Min (g/min)	48.72	21.76	19.20	0.30	63.52	22.74	34.1

[a] Two 30s samples have been averaged to match the 60s sample used in exp. 4.
[b] Ratio of standard deviation based on 60s sampling interval to the standard deviation based on the 30s interval.
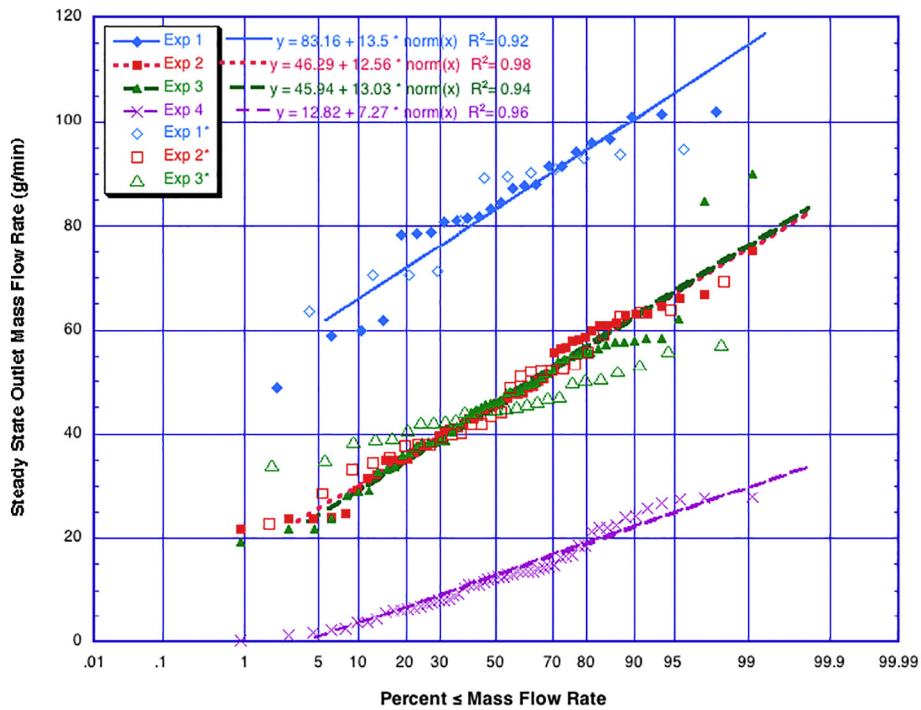
Fig. 4. Normal probability plot of steady state mass flow rates. The asterisk indicates that two 30s samples have been averaged to match the 60s sample used in experiment 4.

mass flow rates increase with the rotation rate of the input airlock. As expected, the mean mass flow rate is essentially directly proportional to the rotation rate since the input airlock meters the feedstock into the reactor. Given a 6-chambered airlock with a chamber volume of 273 cm^3 and a feedstock bulk density of 183 kg/m^3, we would expect the slope between the mean steady state mass flow rate and the airlock rotation rate to be about 300 g/rev, which is within 10% of the observed value.

Several factors may contribute to the observed variation in the steady state mass flow rate. Probably most importantly, the mass flow rate is measured by collecting the material exiting the outlet airlock over a discrete time interval. Specifically, experiment 4 used a 60s

collection interval in contrast to the 30s interval used in the other experiments. Notably, the standard deviation of the mass flow rates measured in experiment 4 is approximately 50% of the standard deviations observed for the other experiments. If two 30s samples are combined to produce a 60s sample for the other experiments, the standard deviations of the mass flow rates for experiments 1 through 3 are all reduced, as shown in Table 3. Since the sample sizes for experiments 1 and 2 were even numbers, combining the two 30s samples into one 60s sample does not change the sample means but does change the sample medians and standard deviations. The distributions of these 60s sample interval results are shown in Fig. 4 as open symbols. The reduction in the standard deviation is expected since the standard
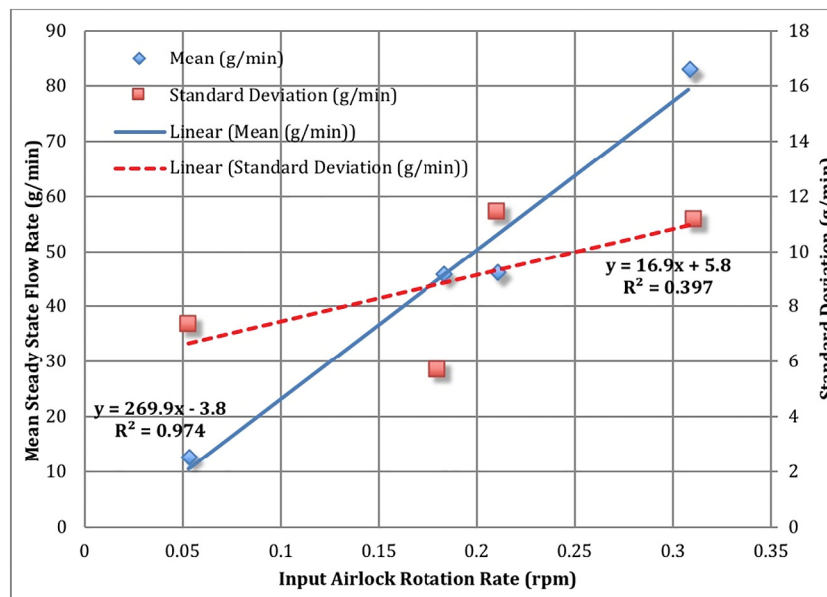

Fig. 5. Mean and standard deviation of steady state mass flow rates vs. input airlock rotation rate.
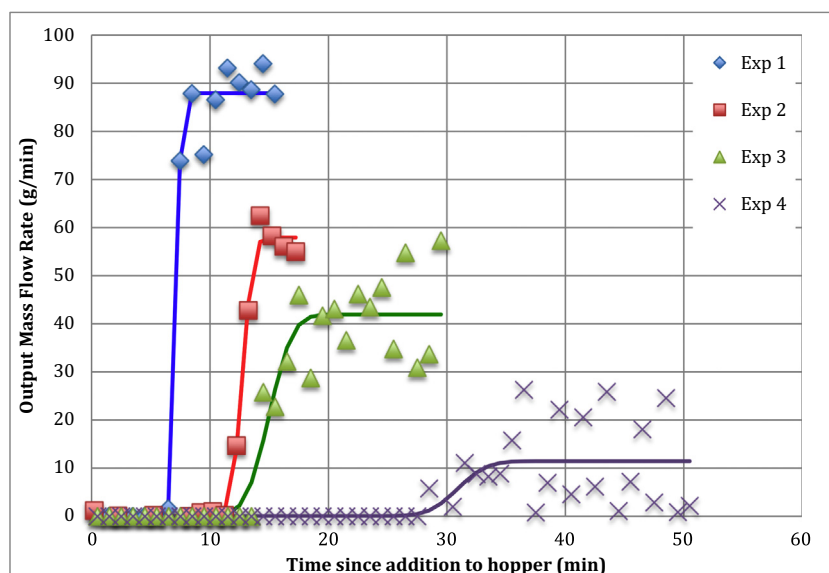
Fig. 6. Observed and predicted response in output mass flow rate to positive step change in input mass flow rate.

deviation of the sample mean is inversely proportional to the square root of the sample size. For a sample size of 2 (i.e., combining two 30s samples into one 60s sample), the expected standard deviation should be about 70% of the original value, which is consistent with the observed average reduction in the standard deviations of 71%.

However, even with the longer sample interval, the standard deviations of the mass flow rates for experiments 1 and 2 remain about twice as large as for experiments 3 and 4. As already discussed in the prior section, another factor that may contribute to the variability in the mass flow rates is that the additions of the feedstock from the input airlock to the screw conveyor and the removals of feedstock through the output airlock occur periodically, not continuously.

4.3. Method A - positive step change

Fig. 6 presents the observed response in the mass flow rate exiting the system to a positive step change in the reactor mass input rate from zero to a steady state mass flow rate ($\dot{m}_{SS,A}$). These datasets began with the first addition of feedstock to the hopper and ended with reaching steady state. All four of the experiments exhibit a sigmoidal arrival curve with considerable variability in the steady state mass flow rate, supporting the assumption of a normal distribution of residence or arrival times. Fig. 6 also shows the predicted response curves for each experiment, based on selecting values of $\dot{m}_{SS,A}$, $\bar{t}_A$, and $S_{t,\,A}$ in Eq. (7) to minimize the sum of squared errors in the mass flow rate (i.e., predicted – observed).

The smaller values of $S_{t,\,A}$ estimated for the shorter residence time experiments indicate less variation or higher precision in the arrival times. The observed increase in scatter of the measured mass flow rates at steady state with the increase in the residence time is likely the result of more back-spill or reverse flow of the material.

Table 4 provides the estimates and standard errors of the estimate for $\dot{m}_{SS,A}$, $\bar{t}_A$, and $S_{t,\,A}$ for each experiment. The standard error in the estimate of $\dot{m}_{SS,A}$ is positively correlated to the standard deviation and range of $\dot{m}_{SS}$ at steady state. The coefficients of variation of the parameter estimates generally increase with the magnitude of the parameter estimate. The observed variability in the mass flow rate after reaching steady state is discussed below in a subsection titled Steady State Mass Flow Rate.

The estimated mean residence times are 0.5 to 2.5 min shorter than the ideal values (i.e., 4% to 8% shorter). These differences all exceed the standard error in $\bar{t}_A$ by at least a factor of 1.8, indicating that it is

Table 4
Estimated RTD parameters based on positive step change.

Parameter	1	2	3	4
Sample size	17	19	31	51
Steady state mass flow rate, $\dot{m}_{SS,A}$ (g/min)	88.0	57.9	42.0	11.5
Average residence time, $\bar{t}_A$ (min)	7.14	12.73	14.99	30.91
Standard dev. of residence time, $S_{t,\,A}$ (min)	0.32	0.70	1.55	1.94
Ideal residence time, τ_{ideal} (min)	7.61	13.60	15.68	33.43
$\bar{t}_A/\tau_{ideal}$	0.94	0.94	0.96	0.92
Standard error in $\dot{m}_{SS,A}$ (g/min)	1.45	0.93	1.82	1.40
Standard error in $\bar{t}_A$ (min)	0.114	0.053	0.370	1.361
Standard error in $S_{t,\,A}$ (min)	0.111	0.068	0.514	1.893
SS sample size	8	4	10	14
Standard dev. in $\dot{m}_{SS}$ (g/min)	5.80	3.31	8.92	9.65
Range in $\dot{m}_{SS}$ (g/min)	18.9	7.5	26.4	25.1

unlikely that the differences are solely due to chance.

4.4. Method B - pulse addition of tracer

Fig. 7 shows the observed mass fraction of the tracer measured in each output sample plotted against the elapsed time since the addition of the tracer pulse to the inlet airlock (i.e., the residence or arrival time). These datasets began with the addition of tracer to the empty hopper and ended when the no more tracer was observed exiting the outlet airlock. All four of the experiments exhibit a somewhat bell-shaped arrival curve with a long trailing tail.

Fig. 8 displays the residence times plotted as a normal probability plot against the observed cumulative RTD function. Except for the long trailing tails of the distributions, the arrival times follow the linear pattern expected for a normal distribution. The start of the tail was identified as the break point where the residence times begin to deviate from the linear trend. The regression lines shown are for the portion of the distribution well-characterized as normal (i.e., the linear portion).

Table 5 summarizes the mean and standard deviation of the residence times for each experiment estimated from the results of the pulse tracer addition. All three of the alternative estimators for the mean residence time yield values within 5% of the average of the three estimates (i.e., $\bar{t}_{B,1} + \bar{t}_{B,2} + \bar{t}_{B,3}$) but were from 9% to 29% longer than the ideal residence times. As expected, omitting the tails of the arrival curves reduces the average residence time. All of these differences in residence time are at least 11 times the standard errors of $\bar{t}_{B,2}$, indicating
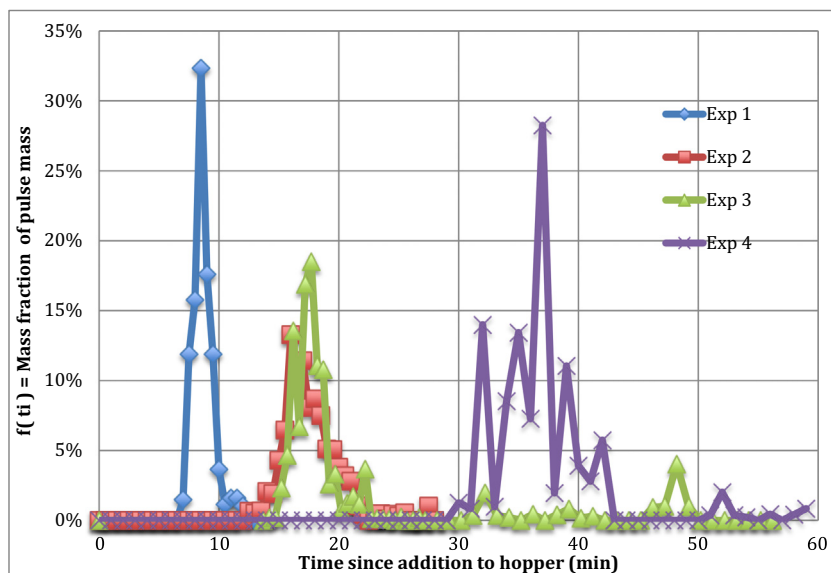
Fig. 7. Observed residence time distributions from four experiments on pulse addition of tracer.

that chance alone cannot explain the difference. The alternative estimators for S_t vary considerably more, but generally increase with average residence time.

The tails of the residence time distributions become increasingly pronounced as the ideal residence times increase. Experiments 1 and 4 have almost identical degrees of fullness but experiment 1, which has a very minor tail, has a screw conveyor rotation rate that is almost three times higher than experiment 4, which has the largest tail. Experiment 2 has a degree of fullness that is twice that of experiment 3, but both have the same have screw conveyor rotation rate. The tail for experiment 3 more pronounced than for experiment 2.

4.5. Method C - negative step change

Fig. 9 presents the observed response in the mass flow rate exiting the system to a negative step change in the reactor mass input rate from the steady state mass flow rate ($\dot{m}_{SS,C}$) to zero. These datasets began when the last tracer has exited the outlet airlock and the hopper has been emptied. All four of the experiments exhibit a sigmoidal arrival curve with considerable variability in the steady state mass flow rate, again supporting the assumption of a normal distribution of residence times. Fig. 9 also shows the predicted response curves for each experiment, based on selecting values of $\dot{m}_{SS,C}$, $\bar{t}_C$, and $S_{t,\,C}$ in Eq. (14) to minimize the sum of squared errors in the mass flow rate (i.e., observed – predicted). The observed variability in the steady state mass flow rate is discussed in the next subsection.
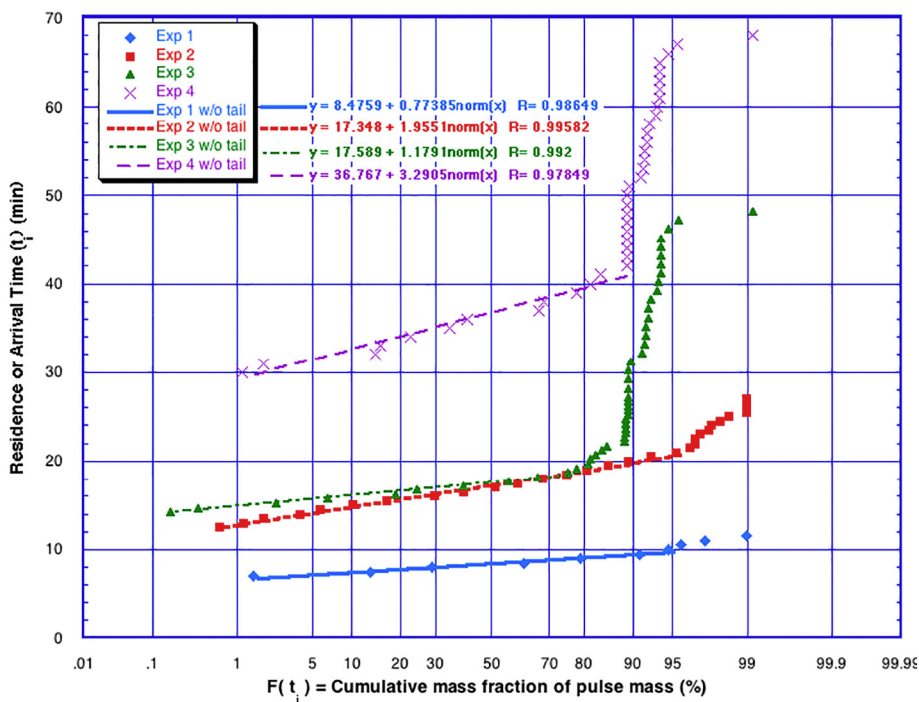

Fig. 8. Normal probability plot of residence time distributions.

Table 5
Estimated RTD parameters based on pulse addition of tracer and comparison of estimates based on all data and data without tails.

Parameter	1	2	3	4	Comments
Sample size	30	10	48	39	
Sample size without tails	18	7	10	13	
Break point for tail (%)	95%	95%	76%	89%	
Average residence time 1, $\bar{t}_{B,1}$ (min)	8.69	17.60	17.84	36.24	All data
Average residence time 1, $\bar{t}_{B,1}$ (min)	8.52	17.21	16.98	35.32	Without tails
Average residence time 2, $\bar{t}_{B,2}$ (min)	8.48	17.35	17.59	36.77	Without tails
Average residence time 3, $\bar{t}_{B,3}$ (min)	8.32	16.95	17.51	36.35	
Ideal residence time, τ_{ideal} (min)	7.61	13.60	15.68	33.43	
$\bar{t}_{B,1}/\tau_{ideal}$	1.14	1.29	1.14	1.08	All data
$\bar{t}_{B,1}/\tau_{ideal}$	1.12	1.27	1.08	1.06	Without tails
$\bar{t}_{B,2}/\tau_{ideal}$	1.11	1.28	1.12	1.10	Without tails
$\bar{t}_{B,3}/\tau_{ideal}$	1.09	1.25	1.12	1.09	
SD residence time 1, $S_{t,B,1}$ (min)	0.90	2.32	5.06	4.04	All data
SD residence time 1, $S_{t,B,1}$ (min)	0.65	1.72	5.68	2.25	Without tails
SD residence time 2, $S_{t,B,2}$ (min)	0.77	1.96	1.18	3.29	Without tails
Standard error of $\bar{t}_{B,2}$	0.07	0.06	0.08	0.24	Without tails
Standard error of $S_{t,B,2}$	0.06	0.05	0.05	0.21	Without tails

Table 6
Estimated RTD parameters based on negative step change.

Parameter	1	2	3	4
Sample size	14	40	25	46
Steady state mass flow rate, $\dot{m}_{SS,C}$ (g/min)	82.2	46.7	46.0	12.9
Average residence time, $\bar{t}_C$ (min)	10.07	32.02	17.32	53.27
Standard dev. of residence time, $S_{t,C}$ (min)	0.41	4.08	0.44	1.72
Ideal residence time, τ_{ideal} (min)	7.61	13.60	15.68	33.43
$\bar{t}_A/\tau_{ideal}$	1.32	2.35	1.10	1.59
Standard error in $\dot{m}_{SS,C}$ (g/min)	7.14	1.49	1.34	0.99
Standard error in $\bar{t}_C$ (min)	0.369	0.636	0.183	1.702
Standard error in $S_{t,C}$ (min)	1.390	0.930	0.206	2.417
SS sample size	10	18	17	39
Standard dev. in $\dot{m}_{SS}$ (g/min)	24.59	7.98	6.46	6.62
Range in $\dot{m}_{SS}$ (g/min)	81.4	17.0	25.6	27.5

is the difference in the degree of fullness (α) between experiments 2 and 3, where experiment 2 that had an 84% longer residence time also had twice the degree of fullness of experiment 3.

4.6. Comparison of RTD parameter estimates

Table 6 summarizes the estimates and standard errors of the estimates for $\dot{m}_{SS,C}$, $\bar{t}_C$, and $S_{t,C}$ for each experiment. The standard error in the estimate of $\dot{m}_{SS,C}$ is positively correlated to the standard deviation and range of $\dot{m}_{SS,C}$ at steady state. The coefficients of variation of the parameter estimates generally increase with the magnitude of the parameter estimate.

The estimated mean residence times are 2.5 to 20 min longer than the ideal values (i.e., 10% to 135% longer). These dramatic differences all exceed the standard error in $\bar{t}_C$ by large factors, indicating that it is highly unlikely that the differences are solely due to chance.

It is also notable that although the ideal residence times for experiments 2 and 3 are similar (i.e., 14 and 16 min, respectively), their estimated mean residence times differ by about 15 min with the value for experiment 2 being 84% larger than that for experiment 3. This contrasts with the results obtained using the positive step change or the pulse tracer data, where the estimated residence times for the two experiments differed from each by < 2.25 min. One possible explanation

In Fig. 10, the average residence times estimated from responses to the pulse addition of tracer ($\bar{t}_{A,2}$), the positive step change ($\bar{t}_B$), and the negative step change ($\bar{t}_C$) are compared to the ideal residence time computed from the airlock and screw conveyor motor rotation rates. The average residence times estimated from the positive step change were consistently shorter (by 0.5 to 2.5 min) than the ideal while the average residence times estimated from the pulse addition of tracer and the negative step change were consistently longer (by 0.9 to 3.8 min for the tracer and by 1.6 to 19.8 min for the negative step change) than the ideal. Expressed as percentage differences from the ideal residence time, the average residence times estimated from the positive step change were 4% to 8% (averaging 6%) shorter while the average residence times estimated from the pulse addition of tracer were 10% to 28% (averaging 15%) longer and those estimated from the negative step change were 10% to 135% (averaging 59%) longer. Based on a Kruskal-Wallis test [2], we can reject at the 1% significance level the hypothesis that these differences were due solely to chance.

It can be argued that the ideal residence time represents the shortest residence time that could be expected in the absence of forward mixing in the reactor. So the longer than ideal mean residence times estimated
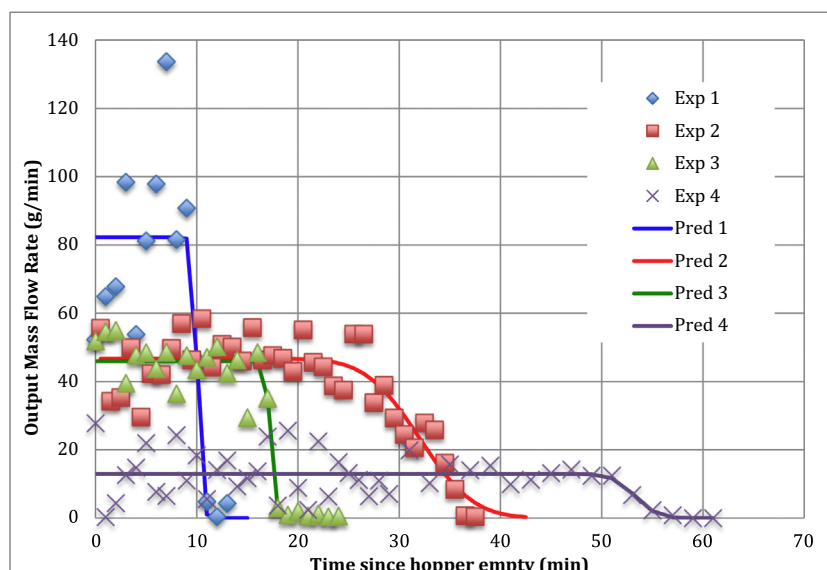

Fig. 9. Observed and predicted response in output mass flow rate to negative step change in input mass flow rate.
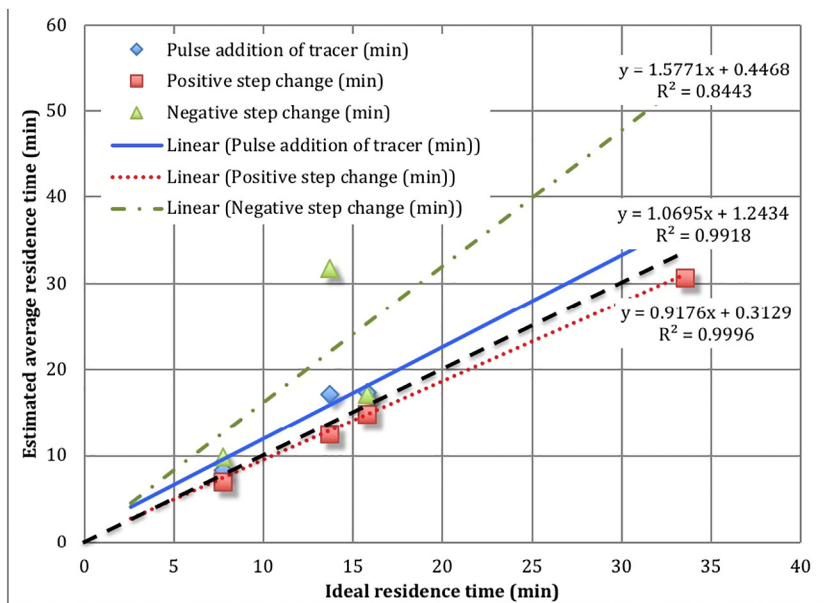
Fig. 10. Ideal residence time compared to the average residence times estimated from the pulse addition of tracer, positive step change, and negative step change. The dashed line is the line of equality with a slope of 1 and an intercept of zero.

from the pulse addition of tracer and the negative step change is not unexpected and are consistent in the direction of the difference with the findings of Nachenius et al. [8] and Waje et al. [10].

The estimated standard deviations of the residence times estimated from the responses to the pulse addition of tracer ($S_{t, A, 2}$), the positive step change ($S_{t, B}$), and the negative step change ($S_{t, C}$) are compared to the ideal residence times in Fig. 11. For the pulse addition of tracer and the positive step change, the estimated standard deviations generally increase with increasing ideal residence time, with coefficients of variation (i.e., the ratio of the standard deviation to the mean) averaging 9% and 7%, respectively. For the negative step change, no clear pattern is apparent, which may be the results of the small sample size and the particularly large mean and standard deviation observed in experiment 2.

4.7. Method advantages and disadvantages

With the pulse tracer, the material flows through the reactor under normal conditions (i.e. the reactor is full with other material), while the positive step change is filling the reactor and the negative step change is emptying the reactor.

For the pulse addition of a tracer, if the tracer matches the density, size, and other characteristics of the feedstock, then the material should flow through the reactor under normal conditions (i.e. the reactor contains a steady state amount of other material) and the residence time distribution for the tracer should match that of the feedstock. The long trailing tail seen in the pulse addition results but not in the negative or positive step results may reflect the normal flow behavior of material in the reactor.

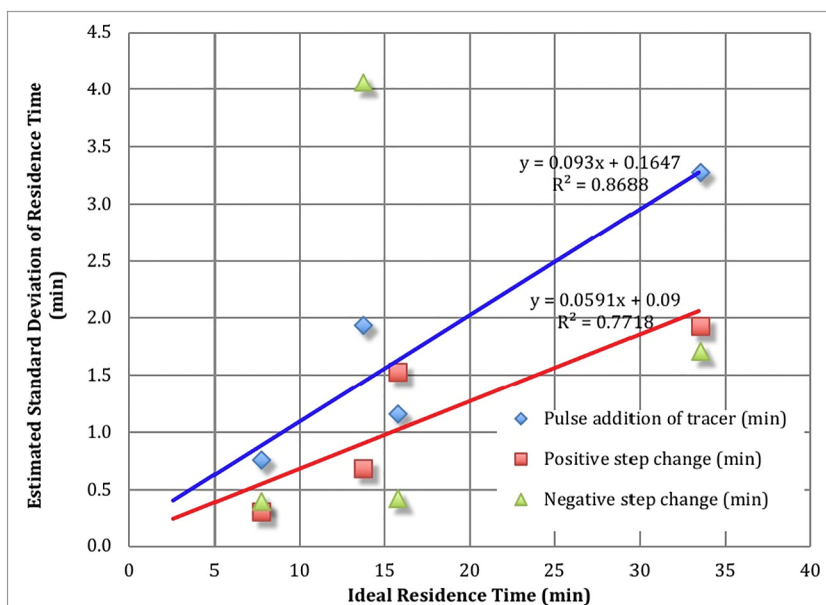The challenge in using a pulse addition is in identifying a tracer that

Fig. 11. Ideal residence time compared to the standard deviation of residence time estimated from the pulse addition of tracer, positive step change, and negative step change.

can tolerate the reactor conditions and in measuring the amount of tracer in each aliquot of material exiting the reactor. The method we used (sorting red-dyed chips by hand) was laborious and time consuming. Waje et al. [10] discuss alternative tracer labels such as water soluble dyes, radioisotopes, magnetic materials, and others. In the experiments described here, the reactor was at ambient temperature but is an active system the tracer would need to tolerate temperatures of 250 to 300 °C for periods of up to 60 min.

The positive step change method is easy to implement whenever the reactor is started from empty. The exiting material must only be collected and weighed at timed intervals. The reactant is used directly and so does not require modification. However, the flow characteristics of the material may be different during the filling process, possibly allowing some material to reach the exit more quickly than under normal operating conditions. Moreover, in an active system some mass is lost to gas production and the amount of mass lost would depend on the reactor residence time and temperature. Consequently, variation in the reactor temperature would cause some random or systematic variation in the mass flow rate. Note that in the experiments described here, the observed average residence times are shorter than for the tracer. The substantial variability in the steady state mass flow rates complicated the analysis of the residence time distribution by this method.

The negative step change method is also easy to implement at the end of a run and has some of the same advantages and disadvantages as the positive step change. But the observed average residence times are longer than for the tracer, possibly because some of the material may have remained in the reactor at the end of the run or because as the mass of material in the reactor is reduced the flow characteristics change such that there is less back-flow through the gap in the screw conveyor and the residence time appears higher than under normal operating conditions.

5. Conclusions

In this work, we have investigated the residence time distribution of feedstock in a pilot scale torrefaction system incorporating a shaftless screw conveyor to which feedstock is added by a rotary airlock and from which feedstock is removed by a second rotary airlock. Three alternative experimental methods have been used to estimate the residence time distribution: 1) a pulse input of tracer, 2) a positive step change in the reactor mass input rate, and 3) a negative step change in the reactor mass input rate.

We compared the residence time distributions and their properties obtained by these three methods. All three methods reveal residence time distributions that are approximately normal (i.e., symmetrical and bell-shaped), but the distribution estimated from the pulse input of tracer exhibited a long trailing tail that was not detectable in either the positive or negative step changes, possibly due to reasons discussed above.

Second, we compared alternative methods describing the residence time distribution and for estimating the mean and standard deviation of the residence time. A normal probability plot proved valuable in displaying and analyzing the residence time distribution obtained by the pulse addition of tracer. The graphical display clearly indicates the portion of the residence time distribution that is well approximated as a normal distribution versus the long trailing tail. The slope and intercept for the dataset without the tail provide estimates of both the mean and standard deviation of the residence time and their associated standard errors. No substantial difference was found among the sample mean or sample median residence times computed with all of the data, the sample mean computed without the tails, or the mean estimated from the normal probability plot without the tails.

Finally, we compared the estimated mean residence times obtained by the three methods to the nominal or ideal residence times. All three methods yielded mean residence times that consistently differed from the nominal values. The positive step change averaged 8% shorter, the pulse addition of tracer averaged 7% longer, and the negative step change averaged 60% longer.

We observed that the distributions of the residence times were less scattered and the tails were less pronounced when the average residence times were shorter and the mass flow rates were higher. This suggests that better process control might be achieved by using shorter residence times/higher mass flow rates coupled with more extreme (higher or lower) temperatures. This should produce a more consistent product in heaters, coolers, dryers, torrefiers, gasifiers and other reactors.

Nomenclature

Symbols

$f(t_i)$	observed residence time distribution function ($-$)
$F(t_i)$	observed cumulative residence time distribution function ($-$)
$F_N(z)$	cumulative normal distribution function of the standard normal deviate ($-$)
L	length of the conveyor (m)
m	mass present in reactor (m)
m_i	mass exiting reactor from time t_{i-1} to t_i (kg)
$m_{t,i}$	mass of tracer exiting reactor from time t_{i-1} to t_i (kg)
$\dot{m}_i$	mass flow rate exiting reactor (kg/s)
$\dot{m}_{t,i}$	mass flow rate of tracer exiting reactor (kg/s)
$\dot{m}_{SS}$	steady state mass flow rate exiting reactor (kg/s)
$\widehat{m_i}$	predicted mass flow rate exiting reactor (kg/s)
n	number of data points ($-$)
p	length of the screw flight or pitch (m)
q_{in}	expected number of inlet airlock chambers per flight ($-$)
q_{out}	expected number of outlet airlock chambers per flight ($-$)
S_t	standard deviation of residence or arrival time (s)
t_i	residence or arrival time (s)
$\bar{t}$	mean residence or arrival time (s)
V	reactor volume (m³)
z	standard normal deviate ($-$)

Greek letters

α	degree of fullness or the fraction of the reactor that is filled by solids during operation ($-$)
ρ_b	bulk density of the material (kg/m³),
τ_{ideal}	overall reactor residence time (s)
τ_{sc}	theoretical or ideal residence time in the screw conveyor (s)
ω_{in}	rotation rate of inlet airlock (Hz)
ω_{out}	rotation rate of outlet airlock (Hz)
ω_{sc}	screw conveyor rotation rate (Hz)

Abbreviations

RTD	residence time distribution

References

[1] Y. Bard, Nonlinear Parameter Estimation, Academic Press, New York, 1967.

[2] W.H. Beyer (Ed.), CRC Handbook of Tables for Probability and Statistics, 2nd edition, CRC Press, Inc., Boca Raton, FL, 1968.

[3] A.S. Bongo Njeng, S. Vitu, M. Clausse, J.-L. Dirion, M. Debacq, Effect of lifter shape and operating parameters on the flow of materials in a pilot rotary kiln: part I. Experimental RTD and axial dispersion study, Powder Technol. 269 (2014) 554–565.

[4] B. Colin, J.-L. Dirion, P. Arlabosse, S. Salvador, Wood chips flow in a rotary kiln: experiments and modeling, Chem. Eng. Res. Des. 98 (2015) 179–187.

[5] A. Kumar, G.M. Ganjyal, D.D. Jones, M.A. Hanna, Modeling residence time distribution in a twin-screw extruder as a series of ideal steady-state flow reactors, J. Food Eng. 84 (3) (2008) 441–448.

[6] O. Levenspiel, W.K. Smith, Notes on the diffusion-type model for the longitudinal mixing of fluids in flow, Chem. Eng. Sci. 6 (1957) 227–233.

[7] O. Levenspiel, Chemical Reaction Engineering, 2nd ed., John Wiley and Sons, New York, 1972.

[8] R.W. Nachenius, T.A. van de Wardt, F. Ronsse, W. Prins, Residence time distributions of coarse biomass particles in a screw conveyor reactor, Fuel Process. Technol. 130 (2015) 87–95.

[9] J.W. Tukey, The Practical Relationship Between the Common Transformations of Percentages or Fractions and of Amounts. Technical Report 36, Statistical Research Group, Princeton University, 1960.

[10] S.S. Waje, A.K. Patel, B.N. Thorat, A.S. Mujumdar, Study of residence time distribution in a pilot-scale screw conveyor dryer, Dry. Technol. 25 (2007) 249–259.

[11] S.S. Waje, B.N. Thorat, A.S. Mujumdar, Hydrodynamic characteristics of a pilot-scale screw conveyor dryer, Dry. Technol. 25 (2007) 609–616.